

# Electronic phase separation in lightly-doped $\text{La}_{2-x}\text{Sr}_x\text{CuO}_4$

M. Matsuda

*Advanced Science Research Center, Japan Atomic Energy Research Institute, Tokai, Ibaraki 319-1195, Japan*

M. Fujita and K. Yamada

*Institute for Chemical Research, Kyoto University, Gokasho, Uji 610-0011, Japan*

R. J. Birgeneau

*Department of Physics, University of Toronto, Toronto, Ontario M5S 1A1, Canada*

Y. Endoh

*Institute for Materials Research, Tohoku University, Katahira, Sendai 980-8577, Japan*

G. Shirane

*Department of Physics, Brookhaven National Laboratory, Upton, New York 11973*

(November 7, 2001)

The hole concentration dependence of the magnetic correlations is studied in very lightly-doped  $\text{La}_{2-x}\text{Sr}_x\text{CuO}_4$  ( $x < 0.02$ ), which shows coexistence of a three-dimensional antiferromagnetic (AF) long-range ordered phase and a spin-glass phase at low temperatures. It is found that the spin-glass phase in the coexistence region also shows a diagonal spin modulation as in the pure spin-glass phase in  $\text{La}_{2-x}\text{Sr}_x\text{CuO}_4$  ( $0.02 \leq x \leq 0.055$ ). Below  $x \sim 0.02$  the diagonal stripe structure is the same as that in  $x \sim 0.02$  with a volume fraction almost proportional to hole concentration, suggesting that electronic phase separation of the doped holes occurs so that some regions with hole concentration  $c_h \sim 0.02$  and the rest with  $c_h \sim 0$  are formed. This represents the most direct observation to-date of electronic phase separation in lightly-doped antiferromagnets. Such phase separation has been predicted by a number of theories.

PACS numbers: 74.72.Dn, 75.10.Jm, 75.50.Lk

## I. INTRODUCTION

Extensive neutron elastic scattering studies on lightly-doped  $\text{La}_{2-x}\text{Sr}_x\text{CuO}_4$  have revealed that a diagonal spin modulation, which is a one-dimensional modulation rotated away by  $45^\circ$  from that in the superconducting phase, occurs universally across the spin-glass phase in  $\text{La}_{2-x}\text{Sr}_x\text{CuO}_4$  ( $0.02 \leq x \leq 0.055$ ).<sup>1-4</sup> Such diagonal stripes have been predicted theoretically<sup>5-9</sup> and have also been observed in insulating  $\text{La}_{2-x}\text{Sr}_x\text{NiO}_4$ .<sup>10,11</sup> These results lead to the important conclusion that the static magnetic spin modulation changes from being diagonal to parallel at  $x = 0.055 \pm 0.005$ , coincident with the insulator-to-superconductor transition. This establishes an intimate relation between the magnetism and the transport properties in the high-temperature copper oxide superconductors. Another important feature in lightly- and medium-doped  $\text{La}_{2-x}\text{Sr}_x\text{CuO}_4$  ( $0.04 \leq x \leq 0.12$ ) is that the charge density per unit length estimated using a charge stripe model is almost constant throughout the phase diagram, even when the modulation rotates away by  $45^\circ$  at the superconducting boundary. However, at a low value for  $x$  ( $x=0.024$ ) the density appears to increase, approaching 1 hole/Cu as in  $\text{La}_{2-x}\text{Sr}_x\text{NiO}_4$ .

It is unknown whether the stripes persist in very lightly-doped  $\text{La}_{2-x}\text{Sr}_x\text{CuO}_4$  ( $x < 0.02$ ) which shows co-

existence of a three-dimensional (3D) antiferromagnetic (AF) long-range ordered phase and a spin-glass phase at low temperatures. Several possibilities have been discussed theoretically. Some theories predict that dilute holes in an antiferromagnet are unstable against phase separation into a hole-rich and a hole-free phase.<sup>12-15</sup> On the other hand, based on numerical calculations for a simple Hubbard model, the incommensurability of the diagonal incommensurate peaks is predicted to change proportionally with hole concentration.<sup>6</sup>

Elastic neutron scattering measurements in oxygenated  $\text{La}_2\text{CuO}_4$  show that a magnetic Bragg peak, which develops below the 3D AF transition temperature  $T_N \sim 90$  K, decreases in intensity below a re-entrant spin-glass order temperature  $T_m \sim 25$  K.<sup>16,17</sup> This is ascribed to a depression of the 3D AF order because of the re-entrant spin-glass transition. Although it has been shown that two-dimensional (2D) AF correlations develop below  $T_m$ , no detailed study has been performed.

The present elastic neutron scattering study yields important new information on the hole concentration dependence of the magnetic properties in the coexistence region ( $x < 0.02$ ). First we confirmed the re-entrant behavior as described above. It is found that in the reentrant phase diagonal incommensurate peaks develop as in the pure spin-glass phase in  $\text{La}_{2-x}\text{Sr}_x\text{CuO}_4$  ( $0.02 \leq x \leq 0.055$ ). The integrated intensity of the diag-

onal incommensurate peaks that develop below  $T_m$  corresponds closely to that of the  $(1,0,0)$  magnetic Bragg peak lost below  $T_m$ . The most remarkable feature is that the parameters (the incommensurability, the peak widths, and the transition temperature) of the diagonal spin modulation at  $x < 0.02$  are locked at the values in  $x \sim 0.02$  and only the volume fraction of the spin-glass phase monotonically decreases with decreasing hole concentration ( $c_h$ ), suggesting that the doped holes phase separate to form some regions with  $c_h \sim 0.02$  and the rest with  $c_h \sim 0$ . Importantly, this behavior is similar to what was predicted for lightly-doped holes in an antiferromagnet in the absence of long-range Coulomb repulsion.<sup>12–15</sup>

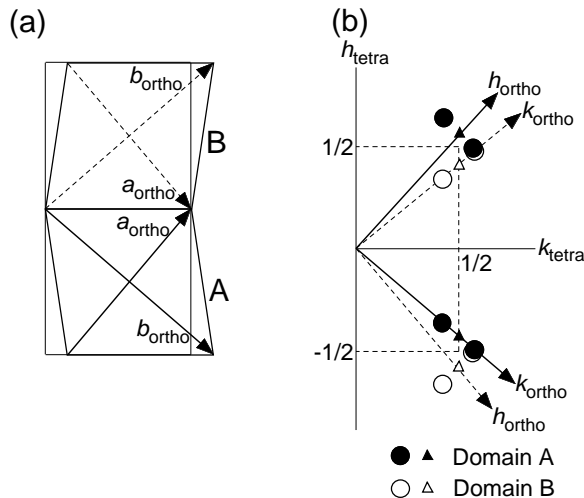


FIG. 1. (a) A schematic drawing of the  $\text{CuO}_2$  planes in the low temperature orthorhombic structure. Two domains (A and B) are shown. The thin lines represent the unit cell in the high temperature tetragonal structure. (b) Diagram of the reciprocal lattice in the  $(HK0)$  scattering zone. Filled and open symbols are for domains A and B, respectively. The circles and triangles correspond to the incommensurate magnetic peaks and fundamental Bragg peaks, respectively.

## II. EXPERIMENTAL DETAILS

The single crystals of  $\text{La}_{2-x}\text{Sr}_x\text{CuO}_4$  ( $x=0.01, 0.014$ , and  $0.018$ ) were grown by the traveling solvent floating zone (TSFZ) method. The crystal was annealed in an Ar atmosphere at  $900^\circ\text{C}$  for 24 h. From the 3D AF transition temperatures, the uncertainty in the effective hole concentration of each crystal is estimated to be less than 10%. The twin structure of the crystals is shown in Fig. 1. As shown in Fig. 2 of Ref. 2, four twins are possible in the low temperature orthorhombic phase ( $Bmab$ ). A small number of twins greatly simplifies the analysis of the incommensurate magnetic peak structure. Fortunately, the  $x=0.010$  and  $0.014$  crystals have almost single domain structures. The  $x=0.018$  crystal has two twins, which are estimated to be equally distributed based on the ratio of the nuclear Bragg peak intensities from both

twins.

The neutron scattering experiments were carried out on the cold neutron three-axis spectrometers LTAS and the thermal neutron three-axis spectrometer TAS2 installed in the guide hall of JRR-3M at the Japan Atomic Energy Research Institute (JAERI). Typical horizontal collimator sequences were guide-80-S-20'-80' with a fixed incident neutron energy of  $E_i=5.05$  meV at LTAS and guide-80'-S-40'-80' with a fixed incident neutron energy of  $E_i=13.7$  meV at TAS2. Contamination from higher-order beams was effectively eliminated using Be filters at LTAS and PG filters at TAS2. The single crystal, which was oriented in the  $(HK0)_{\text{ortho}}$  or  $(HOL)_{\text{ortho}}$  scattering plane, was mounted in a closed cycle refrigerator. In this paper, we use the low temperature orthorhombic phase ( $Bmab$ ) notation  $(h, k, l)_{\text{ortho}}$  to express Miller indices.

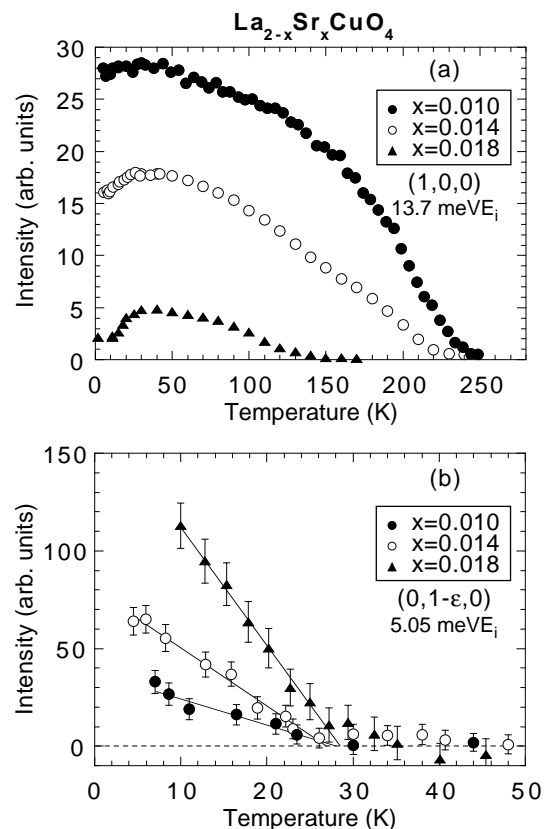


FIG. 2. Temperature dependence of the  $(100)$  magnetic Bragg intensity (a) and the magnetic intensity at the diagonal incommensurate position  $(0,1-\epsilon,0)$  (b) in  $\text{La}_{2-x}\text{Sr}_x\text{CuO}_4$  ( $x=0.01, 0.014$ , and  $0.018$ ). The solid lines are the results of fits to a linear function. Background intensities measured at a high temperature have been subtracted in (b).

## III. RESULTS

Figure 2(a) shows the temperature dependence of the  $(1,0,0)$  magnetic Bragg intensities, originating from the 3D AF order, in  $\text{La}_{2-x}\text{Sr}_x\text{CuO}_4$  ( $x=0.01, 0.014$ , and

0.018).  $T_N$ , as well as the saturated intensity at  $T \sim 30$  K, corresponding to the square of the ordered moment of the  $\text{Cu}^{2+}$  ions, decrease with increasing  $c_h$ . This result is consistent with that in oxygenated  $\text{La}_2\text{CuO}_4$ .<sup>17,18</sup> At a low temperature of  $\sim 30$  K, the magnetic Bragg intensities decrease in the  $x=0.014$  and 0.018 samples and at the same time diagonal incommensurate peaks develop as in the pure spin-glass phase in  $\text{La}_{2-x}\text{Sr}_x\text{CuO}_4$  ( $0.02 \leq x \leq 0.055$ ). As shown in Fig. 2(b), diagonal incommensurate peaks develop below  $\sim 30$  K in all of the samples. The integrated intensity of the incommensurate peaks is calculated using the same method as in Ref. 19. The integrated intensity that develops below  $\sim 30$  K corresponds closely to that of the  $(1,0,0)$  magnetic Bragg peak lost below  $\sim 30$  K, indicating that some regions of the 3D AF ordered phase turn into the diagonal stripe phase.

The diagonal incommensurate peaks have been studied in more detail. As shown in Fig. 2(a), the intense magnetic Bragg peak  $(1,0,0)$  still remains below  $T_m$ , which makes the measurement of the incommensurate  $(1, \pm\epsilon, 0)$  peaks difficult. Therefore, the elastic measurements are performed around  $(0,1,0)$  of domain A where no magnetic Bragg peak exists. Although a small peak originating from a tail of the  $(1,0,0)$  magnetic Bragg peak of the domain B exists near  $(0,1+\epsilon,0)$ : see the small open triangle in lower part of Fig. 1(b), the small background peak can be easily removed by subtracting high temperature data above  $T_m$ . Figure 3 shows elastic scans along  $(0, K, 0)$ . All of the samples clearly show the diagonal incommensurate structure. The peak profiles differ between the  $x=0.010$  and 0.014 samples and the  $x=0.018$  sample. The two peaks are symmetric in the  $x=0.010$  and 0.014 samples because the domain structure is almost single. On the other hand, the two peaks are antisymmetric in the  $x=0.018$  sample because of the nearly two-twin-structure.<sup>20</sup> The solid lines in Fig. 3 are the results of fits to a convolution of the resolution function with 3D squared Lorentzians. In the calculation one domain and equally distributed two twin structure are assumed in the  $x=0.010$  and  $x=0.018$  sample, respectively. A two twin structure with an unbalanced distribution is assumed in the  $x=0.014$  sample.

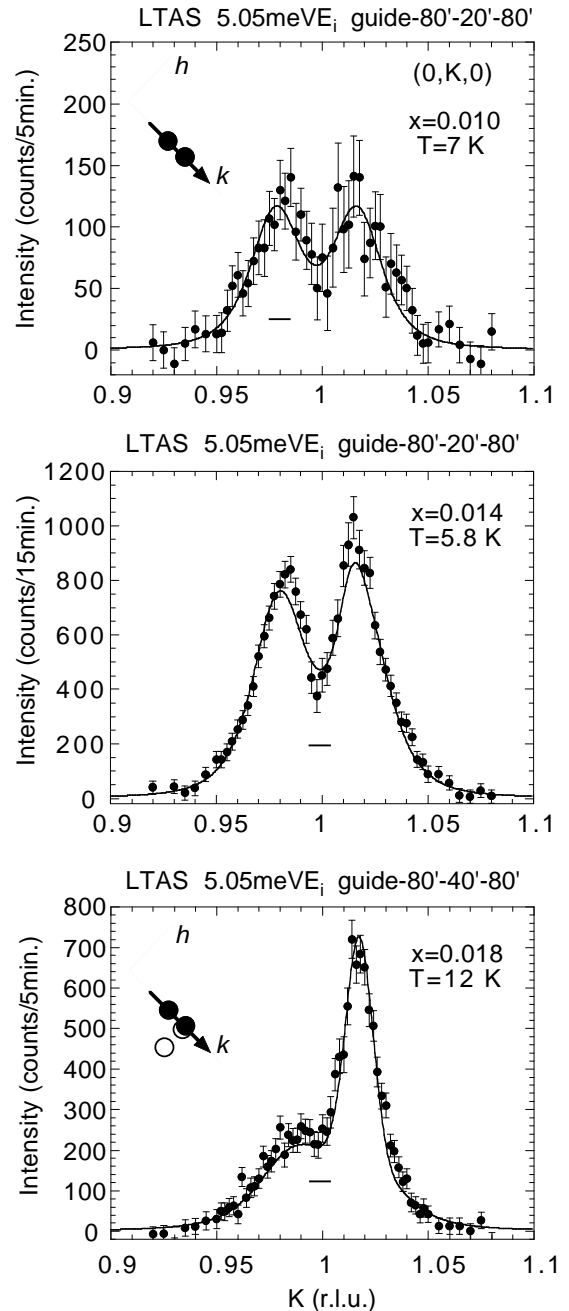


FIG. 3. Elastic scans along  $(0, K, 0)$  in  $\text{La}_{2-x}\text{Sr}_x\text{CuO}_4$  ( $x=0.01, 0.014, \text{ and } 0.018$ ). The data measured above  $T_m$  are subtracted as background intensities. The solid lines are the results of fits to a convolution of the resolution function with 3D squared Lorentzians with the parameters shown in Table 1. The small horizontal bar in each figure represents the instrumental resolution full width. The insets show the magnetic peak positions around  $(0,1,0)$  in the  $(HK0)$  scattering plane. The thick arrows show scan trajectories.

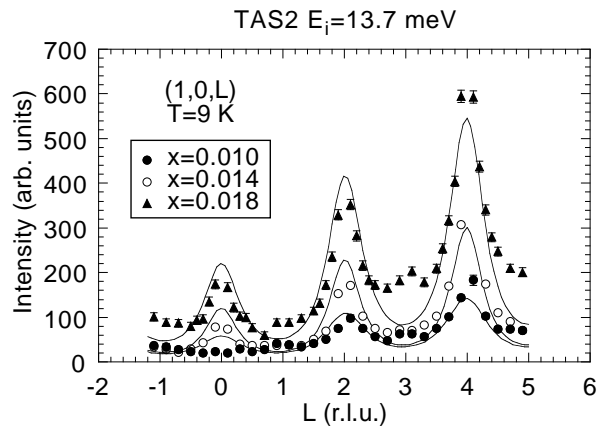


FIG. 4. Elastic scans along  $(1,0,L)$  at  $T=9$  K in  $\text{La}_{2-x}\text{Sr}_x\text{CuO}_4$  ( $x=0.01, 0.014, \text{ and } 0.018$ ). Background intensities measured at a high temperature have been subtracted. The solid lines are the results of fits to a convolution of the resolution function with 3D squared Lorentzians with the parameters shown in Table 1.

Figure 4 shows elastic scans along  $(1,0,L)$  perpendicular to the  $\text{CuO}_2$  planes in the three samples. The solid lines in Fig. 4 are the calculated profiles using 3D squared Lorentzian profiles convoluted with the instrumental resolution function. In order to reproduce the  $L$ -dependence of the  $(1,0, \text{even})$  intensity, the cluster spin-glass model<sup>21</sup> has been used in the calculation. The calculation describes the observed profiles in the  $(HK0)$  and  $(H0L)$  zone reasonably well. The fitted parameters are listed in Table 1. The peak profile is anisotropic as in the  $x=0.024$  sample, that is, in the pure spin-glass phase. One characteristic feature is that the peak is very sharp and close to resolution-limited along the  $a$  axis, which is the direction along which the stripes run. The large inverse peak widths of the incommensurate peaks presumably reflect the fact that the background of the diagonal stripe phase is the long-range 3D AF phase, that is, the long-range AF correlations enhance the correlation length of the diagonal stripe phase. Another characteristic feature is that the inverse peak widths ( $\xi_a > 500$  Å,  $\xi_b \sim 200$  Å,  $\xi_c \sim 10$  Å) and the incommensurability ( $\sim 0.019$  r.l.u.) do not depend on hole concentration below  $x < 0.02$ .<sup>22</sup>

A summary of the elastic neutron scattering results is shown in Figs. 5 and 6. Fig. 5(a) shows the hole concentration dependence of  $T_N$  and  $T_m$ , where  $T_m$  is calculated assuming that the intensity increases linearly below the temperature.  $T_N$  gradually decreases with increasing  $c_h$ . On the other hand,  $T_m$  is constant at  $\sim 28$  K for  $x < 0.02$  and decreases with increasing  $c_h$  at  $x > 0.02$ . As shown in Fig. 6, the incommensurability  $\epsilon$  is locked around 0.02 below  $x=0.02$  and then follows the relation  $\epsilon=x$  in a narrow region around  $x \sim 0.02$  and finally follows the relation  $\epsilon > x$  above  $x=0.03$ .<sup>23</sup> The incommensurability corresponds to the inverse modulation period of the spin density wave. In the diagonal charge stripe model, the relation  $\epsilon=x$  corresponds to a constant charge per unit

length 1 hole/Cu. On the other hand, the relation  $\delta = x$ , where  $\delta$  is in the high temperature tetragonal notation and  $\epsilon = \sqrt{2} \times \delta$ , corresponds to 0.7 hole/Cu, indicating that some of the doped holes are located between the charge stripes. The ordered moment of the  $\text{Cu}^{2+}$  ions in the 3D AF phase at 30 K quickly decreases with increasing  $c_h$  as shown in Fig. 5(b). The  $\text{Cu}^{2+}$  moment in the diagonal spin-glass phase below  $\sim 30$  K is also plotted in the same figure. If the moment is proportional to  $x$ , it is extrapolated to be  $\sim 0.1\mu_B$  at  $x=0.02$ . Assuming that the  $\text{Cu}^{2+}$  moment is  $0.1\mu_B$  in the spin-glass phase of the coexistence region, the volume fraction of the spin-glass phase can be estimated as in the inset of Fig. 5(b).

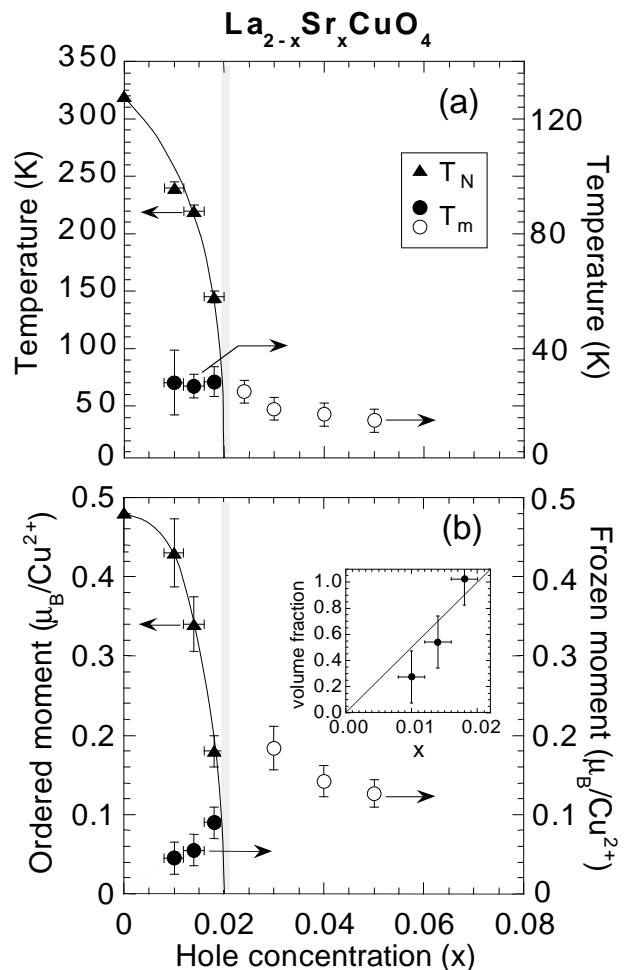


FIG. 5. Hole concentration ( $x$ ) dependence of the magnetic transition temperatures (a) and ordered moment at  $T=30$  K and frozen moment at  $T=4$  K (b).  $T_N$  and  $T_m$  in (a) represent the 3D AF transition temperature and the spin-glass transition temperature, respectively. The inset in (b) shows the estimated volume fraction of the spin-glass phase. Filled symbols in (a) and (b) are determined from the present study. Open symbols in (a) and (b) are from Refs. 4 and 19, respectively. The solid lines are guides-to-the-eyes.

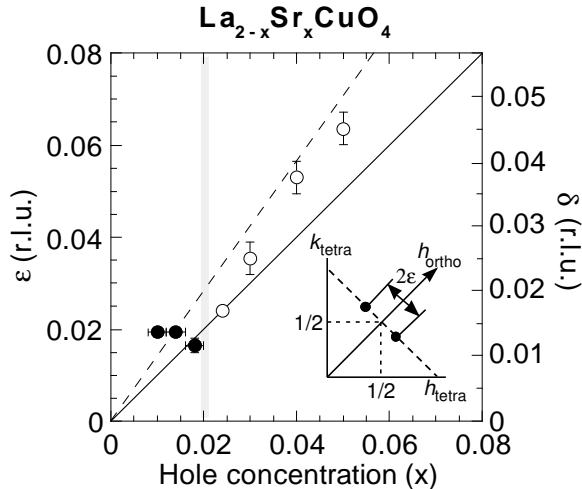


FIG. 6. Hole concentration ( $x$ ) dependence of the splitting of the incommensurate peaks. The inset shows the configuration of the incommensurate peaks in the diagonal stripe phase. Filled symbols are determined from the present study. Open symbols are from Refs. 2 and 3.  $\epsilon = \sqrt{2} \times \delta$  where  $\delta$  is defined in tetragonal units. The solid and broken lines correspond to  $\epsilon = x$  and  $\delta = x$ , respectively.

#### IV. DISCUSSION AND CONCLUSIONS

As shown above, some part of the 3D AF ordered phase turns into the spin-glass phase, in which the stripe structure is almost identical to that at  $x \sim 0.02$ . These results indicate that the doped holes phase separate microscopically to form finite size regions of the  $x=0.02$  stripe phase. Therefore, the hole concentration in the rest of the regions must be much less than  $x$ . If the volume fraction of the spin-glass phase is proportional to  $x$ , the coexistence phase is a mixture of spin-glass phase with  $c_h \sim 0.02$  and 3D AF phase with  $c_h$  close to 0. These results suggest that the transition between the 3D AF and spin-glass phases around  $x=0.02$  is first order and there exists a miscibility gap to form the diagonal stripe. This behavior is predicted for a doped antiferromagnet in the absence of a long-range Coulomb interaction.<sup>12–15</sup> In this study, we determined that  $c_h \sim 0.02$  at the hole-rich region, which was not specified in the theoretical studies. The behavior is much different from that expected from the theory by Kato *et al.*,<sup>6</sup> which has predicted that the incommensurability should follow the relation  $\epsilon=x$  down to very low hole concentrations. Since it is believed that the orthorhombic distortion ( $Bmab$ ) stabilizes the diagonal stripe structure, the crystal structure should favor the stripe structure in the lower hole concentration region. Furthermore, any chemical or structural disorder originating from the Sr doping will decrease with decreasing  $x$ . Therefore, the electronic phase separation of the doped holes must be an intrinsic phenomenon. It is noted that parallel stripes, observed in superconducting  $\text{La}_{2-x}\text{Sr}_x\text{CuO}_4$  ( $x > 0.06$ ), are the most stable at  $x \sim 0.12$

and the incommensurability saturates at  $x > 0.12$ .<sup>25,26</sup> However, no electronic phase separation seems to occur in the  $x > 0.12$  hole concentration region but rather the charge density between charge stripes becomes larger in order to stabilize the stripe periodicity.

We now compare the results of our magnetic study described above with those of previous transport studies.<sup>27,28</sup> It is reported that even in lightly-doped  $\text{La}_{2-x}\text{Sr}_x\text{CuO}_4$  ( $0.01 \leq x \leq 0.03$ ) the in-plane conductivity shows metallic behavior above  $T_L \sim 50\text{-}150$  K. At temperatures below  $T_L$  the doped holes apparently start to localize. Magnetically, our results show that a reentrant spin-glass phase with the diagonal incommensurate structure appears at  $\sim 30$  K. Accordingly, as shown above, hole localization does not seem to occur homogeneously but rather the doped holes form finite size regions with  $c_h \sim 0$  or 0.02 for  $T < 30$  K.

We now compare the results of our neutron scattering study with those of muon spin relaxation ( $\mu\text{SR}$ ) and nuclear quadrupole resonance (NQR) studies.<sup>24,29</sup> It has been found that a static internal field, determined from both  $^{139}\text{La}$  NQR and  $\mu\text{SR}$ , develops below  $T_N$  with a further increase at  $T \sim 30$  K, and the latter temperature does not depend on the hole concentration. The two characteristic temperatures are consistent with those determined from our neutron scattering studies. Furthermore, the internal field at  $T=0$  K appears to be independent of the hole concentration, suggesting that the ordered moment is also independent of hole concentration. This is consistent with our result that the hole concentration of the 3D AF phase becomes almost zero at  $T=0$  K as shown above. On the other hand, the NQR studies show that the spin-glass transition temperature  $T_f$ , determined from the occurrence of a sharp peak in the nuclear spin-lattice relaxation rate as a function of temperature, follows the relation  $T_f \propto x$  below  $x < 0.02$ . This result is different from that in the neutron scattering studies. One possibility is that  $T_f$  depends directly on the volume fraction of the spin-glass phase since our neutron scattering studies show that the volume fraction of the spin-glass phase decrease almost linearly with decreasing  $c_h$ .<sup>30</sup>

TABLE I. Hole concentration dependence of the inverse peak widths in  $\text{La}_{2-x}\text{Sr}_x\text{CuO}_4$ .

$x$	$\xi'_a$ ( $\text{\AA}$ )	$\xi'_b$ ( $\text{\AA}$ )	$\xi'_c$ ( $\text{\AA}$ )
0.010	>500	170(10)	8(2)
0.014	>500	200(10)	9(2)
0.018	>500	170(20)	11(1)
0.024 <sup>a</sup>	95(4)	40(1)	3.15(8)

<sup>a</sup>Ref. 3.

In summary, our neutron scattering experiments demonstrate the electronic phase separation of the doped holes in lightly-doped  $\text{La}_{2-x}\text{Sr}_x\text{CuO}_4$ , which is predicted for a doped antiferromagnet. Some clusters with  $c_h \sim 0.02$  exhibit diagonal stripe correlations while the rest of the crystal with  $c_h \sim 0$  shows 3D AF order.

### ACKNOWLEDGMENTS

We would like to thank K. Ishida and S. Wakimoto for stimulating discussions. This study was supported in part by the U.S.-Japan Cooperative Program on Neutron Scattering, by a Grant-in-Aid for Scientific Research from the Japanese Ministry of Education, Science, Sports and Culture, by a Grant for the Promotion of Science from the Science and Technology Agency, and by CREST. Work at Brookhaven National Laboratory was carried out under Contract No. DE-AC02-98CH10886, Division of Material Science, U.S. Department of Energy. Work at the University of Toronto is part of the Canadian Institute for Advanced Research and is supported by the Natural Science and Engineering Research Council of Canada.

---

<sup>1</sup> S. Wakimoto, R. J. Birgeneau, Y. Endoh, P. M. Gehring, K. Hirota, M. A. Kastner, S. H. Lee, Y. S. Lee, G. Shirane, S. Ueki, and K. Yamada, *Phys. Rev. B* **60**, R769 (1999).  
<sup>2</sup> S. Wakimoto, R. J. Birgeneau, M. A. Kastner, Y. S. Lee, R. Erwin, P. M. Gehring, S. H. Lee, M. Fujita, K. Yamada, Y. Endoh, K. Hirota, and G. Shirane, *Phys. Rev. B* **61**, 3699 (2000).  
<sup>3</sup> M. Matsuda, M. Fujita, K. Yamada, R. J. Birgeneau, M. A. Kastner, H. Hiraka, Y. Endoh, S. Wakimoto, and G. Shirane, *Phys. Rev. B* **62**, 9148 (2000).  
<sup>4</sup> M. Fujita, K. Yamada, H. Hiraka, P. M. Gehring, S. H. Lee, S. Wakimoto, and G. Shirane, *Phys. Rev. B* **65**, 64505 (2002).  
<sup>5</sup> K. Machida, *Physica C* **158**, 192 (1989).  
<sup>6</sup> M. Kato, K. Machida, H. Nakanishi, and M. Fujita, *J. Phys. Soc. Jpn.* **59**, 1047 (1990).  
<sup>7</sup> D. Poilblanc and T. M. Rice, *Phys. Rev. B* **39**, 9749 (1989).  
<sup>8</sup> H. Schulz, *J. Phys. (Paris)* **50**, 2833 (1989).  
<sup>9</sup> J. Zaanen and O. Gunnarsson, *Phys. Rev. B* **40**, 7391 (1990).  
<sup>10</sup> J. M. Tranquada, D. J. Buttrey, V. Sachan, *Phys. Rev. B* **54**, 12318 (1996).  
<sup>11</sup> H. Yoshizawa, T. Kakeshita, R. Kajimoto, T. Tanabe, T. Katsufuji, and Y. Tokura, *Phys. Rev. B* **61**, R854 (2000).  
<sup>12</sup> V. J. Emery, S. A. Kivelson, and H. Q. Lin, *Phys. Rev. Lett.* **64**, 475 (1990).  
<sup>13</sup> S. A. Kivelson and V. J. Emery, in *Proceedings of the Los Alamos Symposium – 1993 : Strongly Correlated*

*Electronic Materials*, edited by K. S. Bedell *et al.* (Addison-Wesley, NY, 1994), p. 619.  
<sup>14</sup> C. S. Hellberg and E. Manousakis, *Phys. Rev. Lett.* **78**, 4609 (1997).  
<sup>15</sup> L. P. Pryadko, S. Kivelson, and D. W. Hone, *Phys. Rev. Lett.* **80**, 5651 (1998).  
<sup>16</sup> Y. Endoh, K. Yamada, R. J. Birgeneau, D. R. Gabbe, H. P. Jenssen, M. A. Kastner, C. J. Peters, P. J. Picone, T. R. Thurston, J. M. Tranquada, G. Shirane, Y. Hidaka, M. Oda, Y. Enomoto, M. Suzuki, and T. Murakami, *Phys. Rev. B* **37**, 7443 (1988).  
<sup>17</sup> B. Keimer, N. Belk, R. J. Birgeneau, A. Cassanho, C. Y. Chen, M. Greven, M. A. Kastner, A. Aharony, Y. Endoh, R. W. Erwin, and G. Shirane, *Phys. Rev. B* **46**, 14034 (1992).  
<sup>18</sup> K. Yamada, E. Kudo, Y. Endoh, Y. Hidaka, M. Oda, M. Suzuki, and T. Murakami, *Solid state Commun.* **64**, 753 (1987).  
<sup>19</sup> S. Wakimoto, R. J. Birgeneau, Y. S. Lee, and G. Shirane, *Phys. Rev. B* **63**, 172501 (2001).  
<sup>20</sup> Detailed description of the peak profile in the twin structure is shown in Ref. 3.  
<sup>21</sup> M. Matsuda, R. J. Birgeneau, P. Böni, Y. Endoh, M. Greven, M. A. Kastner, S.-H. Lee, Y. S. Lee, G. Shirane, S. Wakimoto, K. Yamada, *Phys. Rev. B* **61**, 4326 (2000).  
<sup>22</sup> The error for the incommensurability is large in the  $x=0.018$  sample because the peak splitting along  $K$  is difficult to resolve due to the twin structure.  
<sup>23</sup> The error for the incommensurability becomes smaller at lower hole concentrations because the peaks become sharper as shown in Table 1.  
<sup>24</sup> F. Borsa, P. Carretta, J. H. Cho, F. C. Chou, Q. Hu, D. C. Johnston, A. Lascialfari, D. R. Torgeson, R. J. Gooding, N. M. Salem, and K. J. E. Vos, *Phys. Rev. B* **52**, 7334 (1995).  
<sup>25</sup> J. M. Tranquada, J. D. Axe, N. Ichikawa, Y. Nakamura, S. Uchida, and B. Nachumi, *Phys. Rev. B* **54**, 7489 (1996).  
<sup>26</sup> K. Yamada, C. H. Lee, K. Kurahashi, J. Wada, S. Wakimoto, S. Ueki, H. Kimura, Y. Endoh, S. Hosoya, G. Shirane, R. J. Birgeneau, M. Greven, M. A. Kastner, and Y. J. Kim, *Phys. Rev. B* **57**, 6165 (1998).  
<sup>27</sup> N. W. Preyer, M. A. Kastner, C. Y. Chen, R. J. Birgeneau, and Y. Hidaka, *Phys. Rev. B* **44**, 407 (1991).  
<sup>28</sup> Y. Ando, A. N. Lavrov, S. Komiyama, and X. F. Sun, *Phys. Rev. Lett.* **87**, 17001 (2001).  
<sup>29</sup> F. C. Chou, F. Borsa, J. H. Cho, D. C. Johnston, A. Lascialfari, D. R. Torgeson, and J. Ziolo, *Phys. Rev. Lett.* **71**, 2323 (1993).  
<sup>30</sup> The characteristic lengths in Table 1 do not necessarily represent the cluster size of the spin-glass phase. As suggested in Ref. 3, the incommensurate magnetic peaks could be broad because of disorder in both the periodicity and the direction of the stripes. Therefore, those lengths represent the minimum sizes for the clusters.